 SDHM, vol.2, no.2, pp.69-82, 2006

Influence of Surface Treatements on Fatigue Life of a Free Piston Linear Generator Engine Components Using Narrow Band Approach

M. M. Rahman[1], A.K. Ariffin, N. Jamaludin and C. H. C. Haron

Abstract: This paper describes finite element based vibration fatigue analysis techniques to predict fatigue life using the narrow band frequency response approach. The life prediction results are useful for improving the component design at a very early development stage. The approach is found to be suitable for periodic loading but requires very large time records to accurately describe random loading processes. The focus of this paper is to investigate the effects of surface treatments on the fatigue life of the components of free piston linear engine. The finite element modeling and frequency response analysis have been performed using a computer-aided design and a finite element analysis commercial code, respectively. In addition, the fatigue life prediction was carried out using a finite element fatigue analysis commercial code. The Narrow band approach is specially applied to predict the fatigue life of the free piston linear engine cylinder block. It is observed that there is a significant variation between the surface treatments and untreated cylinder block of free piston engine. The obtained results indicate that the nitrided treatment produces the longest life. This approach is capable of determining premature products failure phenomena. Therefore, it can reduce time to market, improve product reliability and customer confidence.

keyword: Vibration fatigue, Finite element, Power spectral density function, Frequency response, Surface treatment.

1 Introduction

The principal surface treatments such as carburizing or carbonitriding, carried out on many mechanical components before their delivery, are aimed to differentiate the response of surface and core to external loading by changing the surface material properties and by introducing appropriate residual stress distribution in order to improve their fatigue and wear behaviour [Benedetti, Fortanari, Hohn, Oster and Tobie (2002)]. Among the different treatments that can be carried out to locally improve the material response and to modify the stress field, which is a combination of case hardening followed with other surface treatments. Due to the case hardening, the nitriding, shot peening improvement of the residual stress profile [Inoue, Maehara and Yamanaka (1989)]. Shot peening followed by case hardening is capable of improving both the microstructure and the residual stress distribution of the components. Usually residual stresses are introduced by shot peening because of the intense plastic deformation in the surface region [Kobayashi, Matsui and Murakami (1998)], which distinguishes between plastic deformation induced by the Hertzian pressure responsible for the subsurface peak, and plastic deformation due to surface hammering which tends to localize the peak on the surface. Depending on whether the plastic deformation takes place on or below the surface, a shift of the residual stress peaks can be observed with respect to the surface.

Fatigue is an important parameter to be considered in the behaviour of components subjected to constant and variable amplitude loading [Torres and Voorwald (2002)]. Fatigue is of great concern for components subject to cyclic stresses, particularly where safety is paramount, as in the components of free piston linear generator engine. It has long been recognized that fatigue cracks generally initiate from free surfaces and that performance is therefore reliant on the surface topology/integrity produced by surface finishing. It is well known that, in service, many more components and structures fail by cyclic than by static loading. The failure by fracture depends on a large number of parameters and vary often develops from particular surface areas of engineering components. Therefore, it is possible to improve the fatigue strength of fatigue components by the application of suitable surface

[1] Department of Mechanical and Materials Engineering, Universiti Kebangsaan Malaysia (UKM). 43600, Bangi, Selangor DE, Malaysia. Phone:+ (6)03-89216012; Fax: + (6)-03-89216040. E-mail: mustafiz@eng.ukm.my, kamal@eng.ukm.my

treatments. Nowadays, manufacturers are utilizing different surface treatments in order to enhance the surface properties of engineering materials. So far, there are various methods which have been employed to improve the fatigue strength, including optimization of geometric design, materials and surface processing such as nitriding, cold rolled, shot peening etc [Rodopoulos, Curtis, Rois and Solisromero (2004)].

The surface treatments have been the most effective and widely used method of introducing compressive residual stresses into the surface of metals to improve the fatigue performance [Novovic, Dewes, Aspinwall, Voice and Bowen (2004)]. The significance of nitrided, cold rolled and shot peened processes as on surface treatments have raised to even greater importance with the advancement of new analysis methods in metal physics and materials science over the past decades. Typical characteristics of nitrided and shot peened surfaces are compressive residual stresses and extremely high dislocation densities in near surface layers resulting from inhomogeneous plastic deformations. In some cases phase transformations occur, leading to additional surface hardening. These microstructural features are generally considered as the reason for inhibited crack initiation and propagation in components which are cyclically loaded [Martin, Altenberger, Scholtes, Kremmer and Oettel (1998)].

The objective of this paper is to study the influence of surface treatments on the high cycle fatigue of vibrating aluminum alloys cylinder block of a two-stroke free piston engine. However, these investigations are essential in order to understand the involvement of microstructural mechanisms of hardening or softening in the wake of service load. Numerical investigations are performed to characterize completely the different induced effects before and after surface treatments. The numerical results are discussed and analysed.

2 Theoretical Basis

The equation of motion of a linear structural system is expressed in matrix format in Eq. 1. The system of time domain differential equations can be solved directly in the physical coordinate system.

$$[M]\{\ddot{x}(t)\} + [C]\{\dot{x}(t)\} + [K]\{x(t)\} = \{p(t)\} \tag{1}$$

where $\{x(t)\}$ is a system displacement vector, $[M]$, $[C]$ and $[K]$ are mass, damping and stiffness matrices, respectively, {p(t)}is an applied load vector.

When loads are random in nature, a matrix of the loading power spectral density (PSD) functions $[S_p(\omega)]$ can be generated by employing Fourier transform of load vector $\{p(t)\}$.

$$[S_p(\omega)]_{m\times m} = \begin{bmatrix} S_{11}(\omega) & \Lambda & S_{1i}(\omega) & \Lambda & S_{1m}(\omega) \\ M & 0 & & \Lambda & M \\ S_{i1}(\omega) & & S_{ii}(\omega) & & S_{im}(\omega) \\ M & \Lambda & & 0 & M \\ S_{m1}(\omega) & \Lambda & S_{mi}(\omega) & \Lambda & S_{mm}(\omega) \end{bmatrix} \tag{2}$$

where m is the number of input loads. The diagonal term $S_{ii}(\omega)$ is the auto-correlation function of load $p_i(t)$, and the off-diagonal term $S_{ij}(\omega)$ is the cross- correlation function between loads $p_i(t)$ and $p_j(t)$. from the properties of the cross PSDs, it can be shown that the multiple input PSD matrix $[S_p(\omega)]$ is a Hermitian matrix.

The system of time domain differential equation of motion of the structure in Eq. 1, is then reduced to a system of frequency domain algebra equations

$$[S_x(\omega)]_{n\times n} = [H(\omega)]_{n\times m}[S_p(\omega)]_{m\times m}[H(\omega)]^T_{m\times n} \tag{3}$$

where n is the number of output response variables. The Tdenotes the transpose of a matrix. $[H(\omega)]$ is the transfer function matrix between the input loadings and output response variables.

$$[H(\omega)] = \left(-[M]\omega^2 + i[C]\omega + [K]\right)^{-1} \tag{4}$$

The response variables $[S_p(\omega)]$ such as displacement, acceleration and stress response in terms of PSD functions are obtained by solving the system of the linear algebra equations in Eq. 3.

3 The Spectral Moments from PSD

The stress power spectra density represents the frequency domain approach input into the fatigue [Bishop and Sherratt (2000)]. This is a scalar function that describes how the power of the time signal is distributed among frequencies [Bendat (1964)]. Mathematically this function can be obtained by using a Fourier transform of the stress time history's auto-correlation function, and its area represents the signal's standard deviation. The power spectral density is the most complete and concise representation of a random process. The statistical properties of a

stationary ergodic process [Rahman, Ariffin, Jamaludin and Haron (2005)], [Crandell and Mark (1973)], [Newland (1993)] ,[Wirsching, Paez and Oritz (1995)] can be computed from a single time history with sufficiently long period. The time average of a random variable $x(t)$ is equal to the expected value of $x(t)$, as defined as

$$E[x(t)] = \int_{-\infty}^{\infty} x(t)\, dt \tag{5}$$

The mean square value of $x(t)$ is $E[x^2(t)] = \int_{-\infty}^{\infty} x^2(t)\, dt$

Correlation function is a measure of the similarity between two random quantities in a time domain τ .For a single record $x(t)$, the autocorrelation $R(\tau)$ of $x(t)$ is the expected value of the product $x(t)x(t+\tau)$:

$$R(\tau) = E[x(t)x(t+\tau)] = \int_{-\infty}^{\infty} x(t)x(t+\tau)\, dt \tag{6}$$

When τ = 0, the definition Eq. 6 reduces to the mean square value.

$$R(0) = E[x^2(t)]$$

For two random quantities $x(t)$and $y(t)$, the cross correlation function is defined as

$$R_{xy}(\tau) = \int_{-\infty}^{\infty} x(t)y(t+\tau)dt = E[x(t)y(t+\tau)] \quad \text{and}$$

$$R_{yx}(\tau) = \int_{-\infty}^{\infty} y(t)x(t+\tau)dt = E[y(t)x(t+\tau)] \tag{7}$$

Then, the autocorrelation function that defines how a single is correlated itself with a time separation

$$R_{xx}(\tau) = \int_{-\infty}^{\infty} x(t)x(t+\tau)dt = E[x(t)x(t+\tau)]$$

The autocorrelation and PSD functions are related by the Fourier transform pair

$$S_{xx}(\omega) = \frac{1}{2\pi}\int_{-\infty}^{\infty} R_{xx}(\tau)e^{-j\omega\tau}d\tau \tag{8}$$

$$R_{xx}(\tau) = \int_{-\infty}^{\infty} S_{xx}(\omega)e^{j\omega\tau}d\omega \tag{9}$$

As S_{xx} is a real even valued function

$$R_{xx}(\tau) = \int_{-\infty}^{\infty} S_{xx}(\omega)\, \cos\omega\tau\, d\omega \tag{10}$$

By differentiating $R_{xx}(\tau)$ several times with respect to τ , the following equations are obtained

$$R'_{xx}(\tau) = R_{x\dot{x}}(\tau) = -\int_{-\infty}^{\infty} \omega S_{xx}(f)\sin\omega\tau\, df \tag{11}$$

$$R''_{xx}(\tau) = -R_{\dot{x}\dot{x}}(\tau) = -\int_{-\infty}^{\infty} \omega^2 S_{xx}(f)\cos\omega\tau\, df \tag{12}$$

$$R'''_{xx}(\tau) = -R_{\dot{x}\ddot{x}}(\tau) = \int_{-\infty}^{\infty} \omega^3 S_{xx}(f)\sin\omega\tau\, df \tag{13}$$

$$R''''_{xx}(\tau) = R_{\ddot{x}\ddot{x}}(\tau) = \int_{-\infty}^{\infty} \omega^4 S_{xx}(f)\cos\omega\tau\, df \tag{14}$$

The moments therefore, define how each of the processes x, x', x'', etc are elated to the other processes when τ =0,

$$\mu_n = \frac{d^n}{d\tau^n}R_{xx}(0) = \frac{d^n}{dt^n}R_{xx}(0) = \int_{-\infty}^{\infty} \omega^n S_{xx}(f)\, df \tag{15}$$

or in terms of the one sided PSD $G(f)$

$$\mu_n = \int_0^{\infty} (2\pi f)\, 2S_{xx}(f)\, df$$

$$= (2\pi)^n \int_0^{\infty} f^n G_{xx}(f)\, df = m_n\,(2\pi)^n \tag{16}$$

where, $m_n = \int_0^{\infty} f^n G_{xx}(f)\, df$

The method for computing these moments is shown in Fig. 1.

It is important to note that μ_1 and μ_3 are zero, but $m_1$and m_3 are not. Remember that μ_n is produced by integrating from -∞ and +∞, and m_n is produced by integrating from 0 and +∞. Typically, we calculate m_0, m_1, m_2, and m_4.

The most common spectral moment is μ_0, which determine the variance of a PSD

$$\mu_0 = \sigma_x^2 = \int_{-\infty}^{\infty} S_{xx}(\omega)\, d\omega = 2\int_0^{\infty} S_{xx}(\omega)\, d\omega$$
$$= \int_0^{\infty} G(f)\, df = m_0 \tag{17}$$

Here μ_0 and $m_0$are equal. The root mean square (rms) value of the zero mean process is given by $\sqrt{m_0}$.

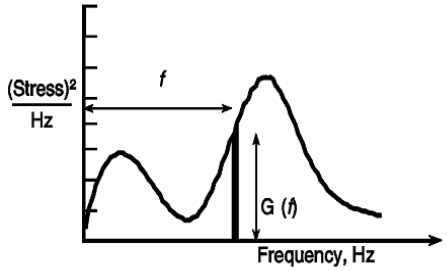

Figure 1 : Calculating moments from a PSD

A more complicated example of the use of these moments considers the number of zero crossings in a stationary random and Gaussian (normal) process. Consider the 2D probability function $p(\alpha, \beta)$ of x and $\dot{x}$

$$p(\alpha,\beta)\Delta\alpha\Delta\beta \approx Prob[\alpha \le x(t) \le \alpha+\Delta\alpha \text{ and } \beta \le \dot{x}(t) \le \beta+\Delta\beta] \tag{18}$$

This probability represents the fraction of time that x is between α and $\Delta\alpha$, when the velocity $\dot{x}$is between $\beta+\Delta\beta$. If the time to cross one interval as Δt.

$$\Delta t = \frac{\Delta\alpha}{|\beta|} \tag{19}$$

From which we can obtain the expected total number of positive crossings of level

$$\frac{p(\alpha,\beta)\Delta\alpha\Delta\beta}{\Delta t} \approx |\beta|\, p(\alpha,\beta)\Delta\beta \tag{20}$$

As $\Delta\beta \to 0$, the total expected number of passages per unit time through $x(t) = \alpha$ for all possible values of β is given by

$$E[\alpha] = \int_0^{\infty} |\beta| p(\alpha,\beta)\, d\beta \tag{21}$$

By setting $\alpha = 0$, we get the required number of zero crossings per unit time

$$E[0] = \int_0^{\infty} |\beta| p(0,\beta)\, d\beta \tag{22}$$

The 2D normal density function of x and $\dot{x}$ is given by

$$p(\alpha,\beta) = (2\pi)^{-1} |A|^{-0.5} e^{\left[\frac{-1}{2|A|}\left(A_{11}\alpha^2 + 2A_{12}\alpha\beta + A_{22}\beta^2\right)\right]} \tag{23}$$

where,

$$A = \begin{bmatrix} a_{11} & a_{12} \\ a_{21} & a_{22} \end{bmatrix} \text{ and } a_{ij} = E[x_i x_j] = a_{ji} \tag{24}$$

The a_{ij} terms are the covariances or second moments of x_i and x_j. The a_{ii} terms are the variances ofx_i and x_j. $|A|$ is the determinant of A and A_{ij} is the cofactor of a_{ij}

we get,

$$a_{11} = R(0) = \mu_0; \quad a_{12} = a_{21} = \mu_1 = 0; \quad a_{22} = \mu_2 \tag{25}$$

Therefore, $A = \begin{bmatrix} \mu_0 & 0 \\ 0 & \mu_2 \end{bmatrix}$

From which we get,

$$E[\alpha] = \frac{1}{2\pi}\left[\frac{\mu_2}{\mu_0}\right]^{\frac{1}{2}} e^{\frac{\alpha^2}{2\mu_0}} \tag{26}$$

If we set $\alpha = 0$, then $E[0] = \left[\frac{m_2}{m_0}\right]^{\frac{1}{2}}$

In a similar way, we can derive results for the number of peaks per unit time is $E[P] = \left[\frac{m_4}{m_2}\right]^{\frac{1}{2}}$

The irregularity factor is $\gamma = \frac{E[0]}{E[P]} = \left[\frac{m_2}{\sqrt{m_0 m_4}}\right]$

The irregularity factor γ is an important parameter that can be used to evaluate the concentration of the process near a central frequency. Therefore, γ can be used to determinate whether the process is narrow band or wide band. A narrow band process ($\gamma \to 1$) is characterized by only one predominant central frequency indicating that the number of peaks per second is very similar to the number of zero crossings of the signal. This assumption leads to the fact that the pdf of the fatigue cycles range is the same as the pdf of the peaks in the signal (Bendat theory). In this case fatigue life is easy to estimate. In contrast, the same property is not true for wide bend process ($\gamma \to 0$). Fig. 2 shows different type of time histories and its corresponding PSD function.

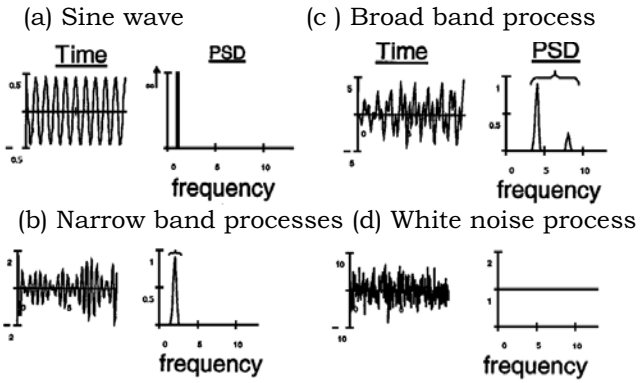

Figure 2 : Equivalent time histories and PSDs.

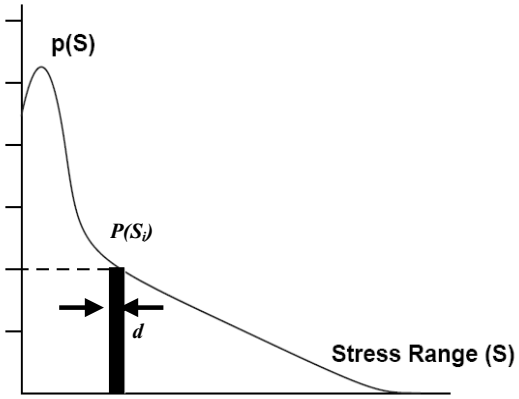

Figure 3 : Probability density functions.

4 Probability Density Functions (pdf's)

The most convenient way of storing stress range histogram information is in the form of a probability density function (pdf) of stress ranges [Bendat (1964)], [Rahman, Ariffin, Jamaludin and Haron (2005)]. A typical representation of this function is shown in Fig. 3. It is very easy to transform the stress range histogram to a pdf form, or backward. The bin widths used, and the total numbers of cycles recorded in the histogram are the only additional pieces of information required. To get a pdf from a rainflow histogram each bin in the rainflow count has to be multiplied by $S_t \times dS$. where $S_t$is the total number of cycles in histogram; dS is the interval width.

The probability of the stress range occurring between S_i-dS/2 and S_i + dS/2 is given by $p(S_i)dS$.

The actual counted number of cycles is equal to $n_i = p(s)\,dS\,S_t$

The allowable number of cycles is given by $N(S_i) = \frac{k}{S^b}$

The damage is then defined by,

$$E[D] = \sum_i \frac{n_i}{N(S_i)} = \frac{S_t}{k}\int S^b p(s)dS \tag{27}$$

Failure occurs, $D \geq 1.0$.

In order to compute fatigue damage over the lifetime of the structure in seconds the form of materials S-N data must also be defined using the parameters k and b. The typical S-N curve as shown in Fig. 4. This figure simply shows that, under constant amplitude cyclic loading, a linear relationship exists between cycles to failure (N) and applied stress range (S) when plotted on log-log paper. There are two alternative ways of defining this relationship, as given in Equation (28). In addition, the total number of cycles in time T must be determined from the number of peaks per seconds $E[P]$. If the damage caused in time T is greater than 1.0 then the structure is assumed to have failed or alternatively the fatigue life can be obtained by setting $E[D]$ =1.0 and then finding the fatigue life T in seconds from the fatigue damage is given by Eq. 27.

$$N = kS^{-b}, \text{ where } b = -\frac{1}{b1}, andk = (SRI1)^b \tag{28}$$

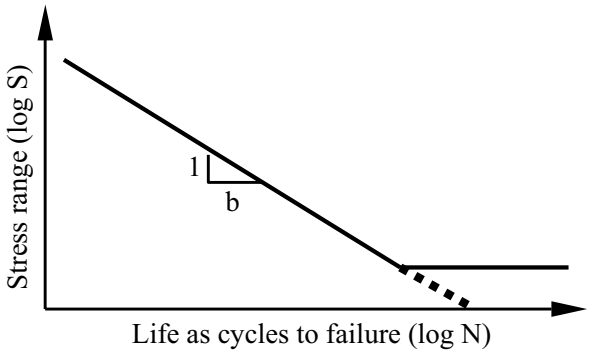

Figure 4 : A Typical S-N curve

5 Narrow Band Solution

Bendat [1964] has proposed first significant step towards a method of determining fatigue life from PSDs, which is so called Narrow band solution. This expression was defined solely in terms of the spectral moments up to m_4.Bendat showed that the probability density function

(pdf) of peaks for a narrow band signal tended towards Rayleigh distributions as the bandwidth reduced. Furthermore, for a narrow band time history, Bendat assumed that corresponding troughs of similar magnitude regardless of whether they actually formed stress cycles would follow all the positive peaks in the time history. Using this assumption the pdf of stress range would also tend to a Rayleigh distribution. To complete the solution method, Bendat used a series of equations derived by [Rice (1954)] to estimate the expected number of peaks using moments of area beneath the PSD. The narrow band formula [Bishop and Sherratt (2000)],[Rahman, Ariffin, Jamaludin and Haron(2005)] is given by the Eq. 29.

$$\begin{aligned} E[D] &= \sum_i \frac{n_i}{N(S_i)} \\ &= \frac{S_t}{K} \int S^b p(S) dS \\ &= \frac{E[P]T}{K} \int S^b [\frac{S}{4.m_0} e^{\frac{s^2}{8m_0}}] \, dS \\ &= E[P]T \left\{ \frac{S}{4m_0} e^{\frac{s^2}{8m_0}} \right\} \end{aligned} \tag{29}$$

This is the first frequency domain method for predicting fatigue damage from PSDs and it assumes that the pdf of the peaks is equal to the pdf of the stress amplitudes. The narrow band solution was then obtained by substitutions the Rayleigh pdf of peaks with the pdf of stress ranges. The full equation is obtained by noting that S_t is equal to $E[P].T$, where T is the life of the structure in seconds. The basis of the narrow band solution is shown in Fig. 5.

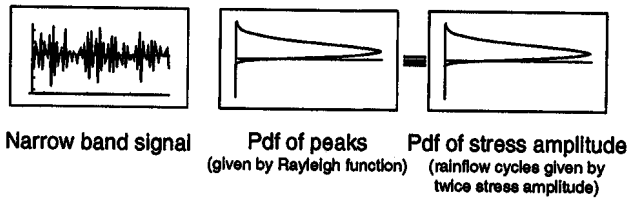

Figure 5 : The Basis of the narrow band solution

6 Application of Linear Generator Engine Component

A geometric model of the cylinder block of the free piston engine is considered in this study. Three-dimensional model of free piston linear engine cylinder block was developed using the CATIA? software. A 10-node tetrahedral element was used for the solid mesh. Sensitivity analysis was performed to obtain the optimum element size. These analyses were performed iteratively at different element lengths until the solution obtained appropriate accuracy. Convergence of stresses was observed, as the mesh size was successively refined. The element size of 0.20 mm was finally considered. A total of 35415 elements and 66209 nodes were generated with 0.20 mm element length. Compressive loads were applied as pressure (7 MPa) acting on the surface of the combustion chamber and preloads were applied as pressure (0.3 MPa) acting on the bolt-hole surfaces. In addition preload was also applied on the gasket surface generating pressure of 0.3 MPa. The Multi-point Constraints (MPCs) were applied on the bolt-hole for all six degree of freedom. Multi-point constraints [Schaeffer (2001)] were used to connect the parts thru the interface nodes. These MPCs were acting as an artificial bolt and nut that connect each parts of the structure. Each MPC's will be connected using a Rigid Body Element (RBE) that indicating the independent and dependent nodes. The configuration of the engine is constrained by bolts to the cylinder head and the cylinder block. In the condition with no loading configuration the RBE element with six-degrees of freedom were assigned to the bolts and the hole on cylinder head. The independent node was created on cylinder block hole. The Pseudo-static and frequency response analyses are performed using MSC.NASTRAN finite element software. The frequency response analysis used a damping ratio of 5% of critical. The damping ratio is the ratio of the actual damping in the system to the critical damping. Most experimental modal analysis software packages report the modal damping in terms of non-dimensional critical damping ratio expressed as a percentage [Formenti (1999)], [Gade, Herlufsen and Konstantin-Hansen (2002)]. In fact, most structures have critical damping values in the range of 0 to 10%, with values of 1 to 5% as the typical range [MSC.Software 2002]. Zero damping ratio indicate that the mode is undamped. Damping ratio of one represents the critically damped mode. The results of Pseudo-static and frequency response finite element analysis at zero Hz i.e. the maximum principal stresses distribution of cylinder block are presented in Fig. 6 and Fig.7 respectively. From the results, the maximum and minimum principal stresses of 38.0 MPa and –7.75 MPa for Pseudo static analysis, and

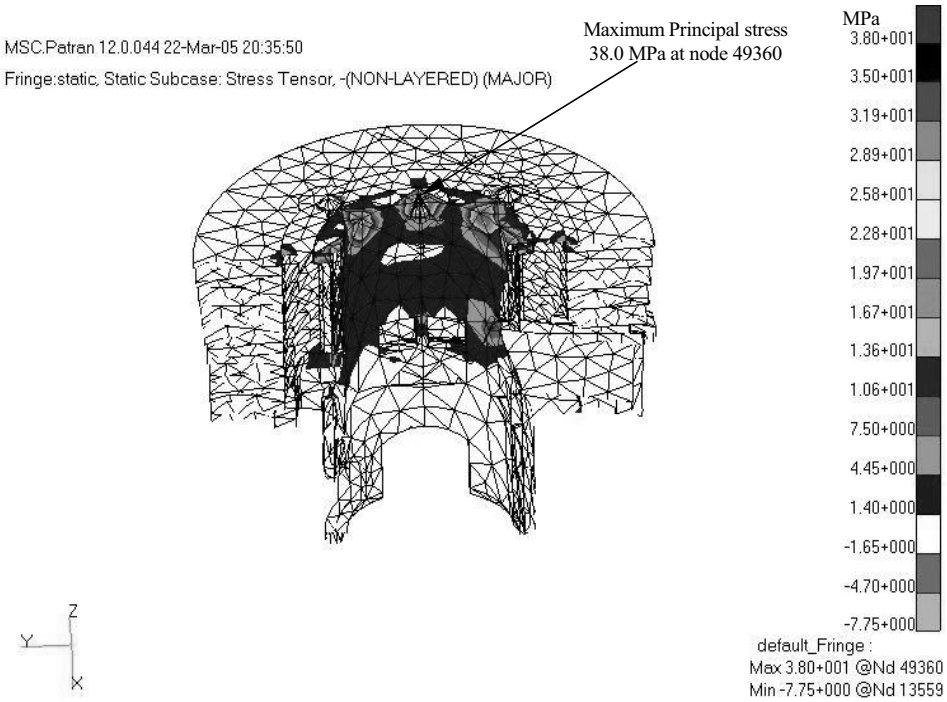

Figure 6 : Maximum principal stresses distribution for linear static analysis

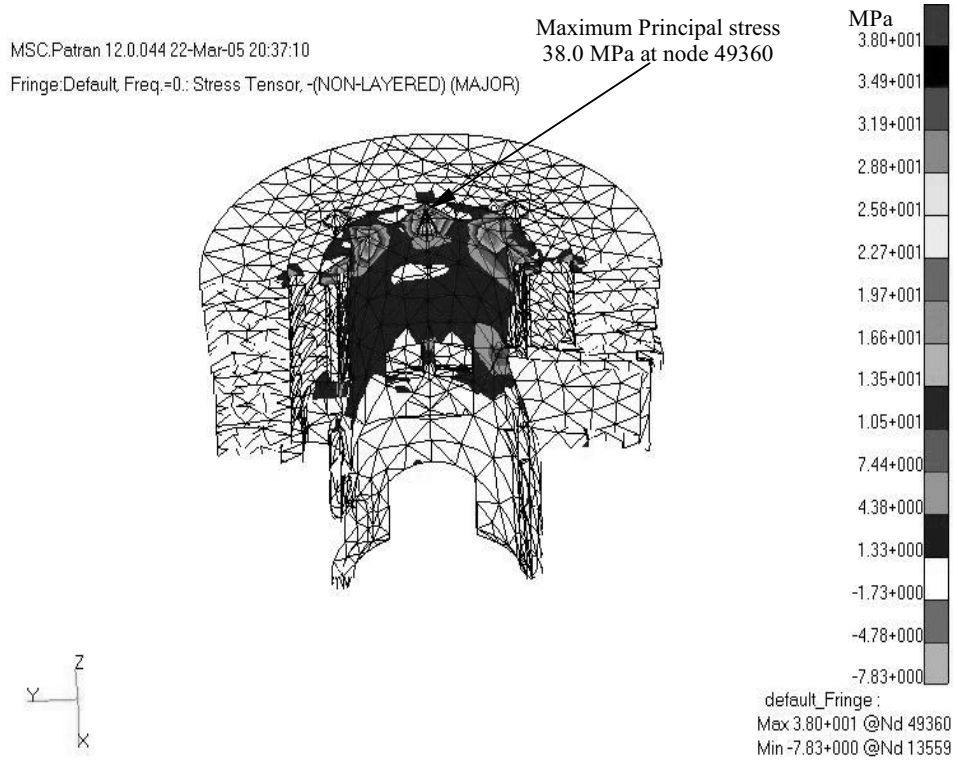

Figure 7 : Maximum principal stresses distribution for frequency response analysis

38.0 MPa and –7.83 MPa for frequency response analysis at zero Hz were obtained respectively. These two contour plots are almost identical.

When the plot are drawn at higher frequencies, it can be shown that a small variation from the static cases. This variation is due to the dynamic influences of the first mode shape. It is shown that the maximum principal stress varies with the higher frequencies. The variation of the maximum principal stresses with the frequency is shown in Fig. 8. It is observed that the maximum principal stress occurs at frequency of 32 Hz.

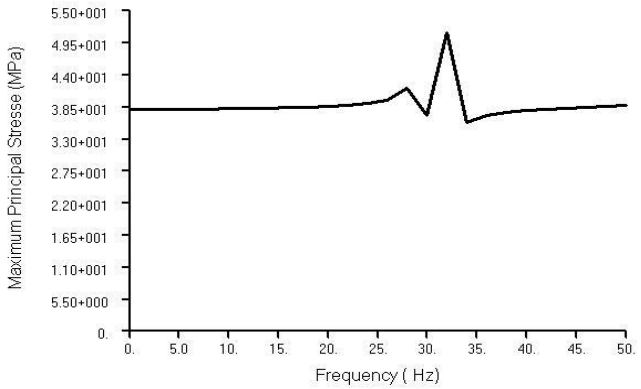

Figure 8 : Maximum principal stresses plotted against frequency

The maximum principal stresses of the cylinder block for 32 Hz is presented in Fig. 9. From the results, maximum and minimum principal stresses of 56.1 MPa at node 50420, and –20.7 MPa at node 47782 were obtained, respectively. Several types of variable amplitude loading histories were selected from the SAE and ASTM profiles for the FE based fatigue analysis. The details information about these histories is given in the literature [Rahman, Ariffin, Jamaludin and Haron (2005)]. The variable amplitude load-time histories are shown in Fig. 10 and the corresponding PSD plot are also shown in Fig. 11. The terms of SAETRN, SAESUS, and SAEBKT represents the load-time history for the transmission, suspension, and bracket respectively [Rahman, Ariffin, Jamaludin and Haron 2005]. The considered load-time histories are based on the SAE's profile. In addition, I-N, A-A, A-G, R-C, and TRANSP are representing the ASTM instrumentation & navigation typical fighter, ASTM air-to-air typical fighter, ASTM air to ground typical fighter, ASTM composite mission typical fighter, and ASTM composite mission typical transport loading history, respectively [Rahman, Ariffin, Jamaludin and Haron (2005)]. The abscissa is the time, in seconds.

The fatigue life contour result for the most critical locations for 32 Hz is shown in Fig. 12 using the SAETRN loading histories [Rahman, Ariffin, Jamaludin and Haron (2005)]. The minimum life prediction is $10^{9.44}$ seconds at node 49360 for 32 Hz and maximum predicted life is $10^{17.4}$ seconds. Tab. 1 shows that the comparison between Pseudo-static and vibration fatigue analysis using narrow band frequency response method for different loading conditions of cylinder block made of AA6061-T6 material. It is observed that there is good agreement between the Pseudo-static and vibration fatigue analysis approaches. The full set of comparison results for untreated polished cylinder block at critical location (node 49360) is given in Tab. 2 with different loading conditions. The Narrow band solution is considered in this study. It is observed that from the Table 2, the SAESUS loading condition gives the longest fatigue life for all materials while A-G loading conditions gives the lowest fatigue life for all materials.

Table 1 : Predicted life in seconds between two approaches at critical location.

Loading Conditions	Pseudo-static	Vibration
SAETRN	1.14×10^{8}	2.10×10^{8}
SAESUS	6.34×10^{9}	8.74×10^{9}
SAEBKT	7.56×10^{7}	1.06×10^{8}
I-N	3.02×10^{9}	6.30×10^{9}
A-A	5.39×10^{8}	3.93×10^{9}
A-G	2.72×10^{7}	3.23×10^{7}
R-C	1.27×10^{8}	3.02×10^{8}
TRANSP	1.15×10^{8}	2.27×10^{8}

The effect of surface treatments on the fatigue life of component subjected to variable amplitude loading conditions was also investigated. The material used in this study was AA6061-T6 and the surface finish was in polished. Surface effects are caused by the differences in the surface roughness, microstructure, chemical composition, and residual stress [Bannantine, Comer and Handrock (1990)]. The correction factor for the surface finish is sometimes used as a qualitative description of the surface finish, such as polished or machined [Bannan-

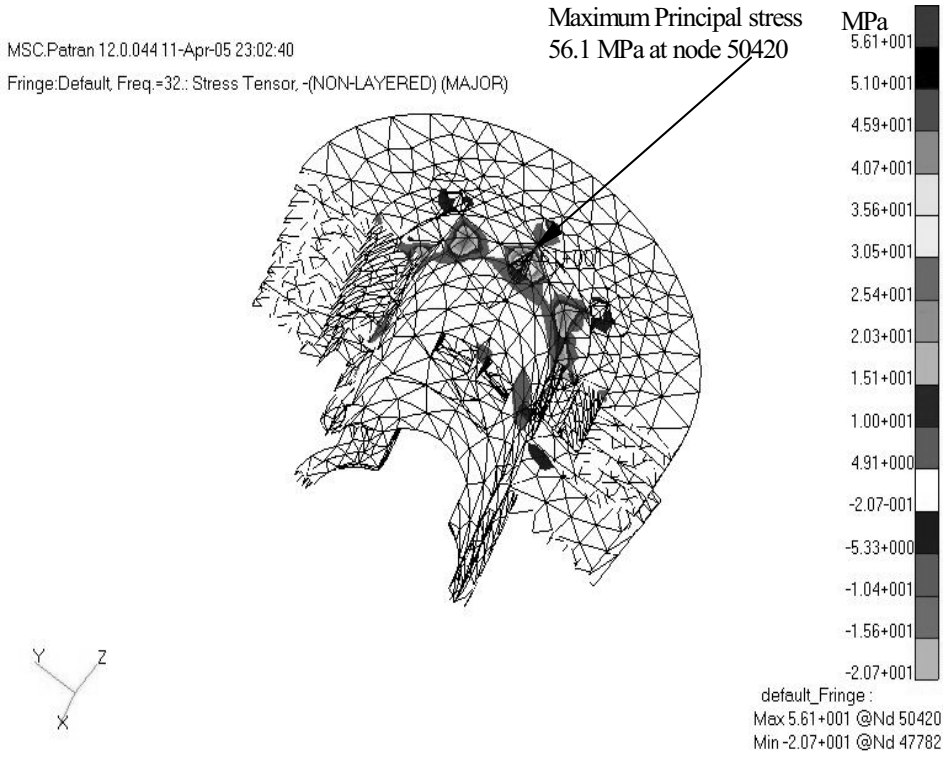

Figure 9 : Maximum Principal stresses contour for 32 Hz

Table 2 : Predicted life in seconds at weakest location (at Node 49360)

Loading conditions	Predicted Life in seconds at critical location (at node 49360)							
	2014-T6	2024-T86	2219-87	5083-87	5454-CF	6061-T6	7075-T6	7175-T73
SAETRN	4.27×10^{7}	1.25×10^{9}	8.48×10^{8}	3.56×10^{7}	1.30×10^{7}	2.10×10^{8}	1.08×10^{10}	2.33×10^{9}
SAESUS	5.01×10^{10}	3.78×10^{12}	3.36×10^{11}	2.51×10^{11}	9.24×10^{10}	8.74×10^{9}	9.51×10^{12}	1.10×10^{15}
SAEBKT	4.96×10^{8}	1.53×10^{10}	9.07×10^{9}	7.78×10^{8}	3.18×10^{8}	1.06×10^{8}	1.59×10^{11}	1.55×10^{11}
I-N	2.64×10^{8}	8.02×10^{9}	4.66×10^{9}	4.52×10^{8}	1.86×10^{8}	6.30×10^{0}	8.52×10^{10}	1.13×10^{11}
A-A	5.99×10^{7}	1.85×10^{9}	1.17×10^{9}	7.08×10^{7}	2.78×10^{7}	3.93×10^{9}	1.76×10^{10}	7.71×10^{9}
A-G	1.66×10^{7}	4.87×10^{8}	3.29×10^{8}	1.40×10^{7}	5.11×10^{6}	3.23×10^{7}	4.21×10^{9}	9.26×10^{8}
R-C	3.19×10^{7}	9.66×10^{8}	6.29×10^{8}	3.19×10^{7}	1.21×10^{7}	3.02×10^{8}	8.78×10^{9}	2.65×10^{9}
TRANSP	1.95×10^{9}	4.99×10^{10}	2.67×10^{10}	5.07×10^{9}	2.07×10^{9}	2.27×10^{8}	5.92×10^{11}	4.20×10^{12}

tine, Comer and Handrock (1990), Stephens, Fatemi, Stephens and Fuchs (2001)]. The surface factors are related to the ultimate tensile strength with different surface finish conditions such as grinding, machining, hot rolling and as forged [Juvinal and Marshek (1991)]. The correction factor for the surface treatments are obtained from [Lipton and Juvinall (1963), Juvinall and marshek (1991), Reemsnyder (1985)] empirical data and are related to the ultimate strength of the material. The effects of surface treatments on the fatigue life at different loading conditions using narrow band frequency response method at critical location are summarized in Tab. 3. Surface treatments including nitriding, cold rolling and shot peening that produced compressive residual surface stresses can prolong the fatigue life. These treatments cause the maximum tensile stress to occur below the surface. However, the tensile residual surface stresses are found to be very detrimental and can be promote corrosion fatigue. In addition, Surface treatments can also increase the endurance limit of the material used. A diffusion process such as nitriding is found to be a very beneficial for increasing the fatigue strength. This process is capable of increasing the strength of the material on the surface as well as causing volumetric changes, which

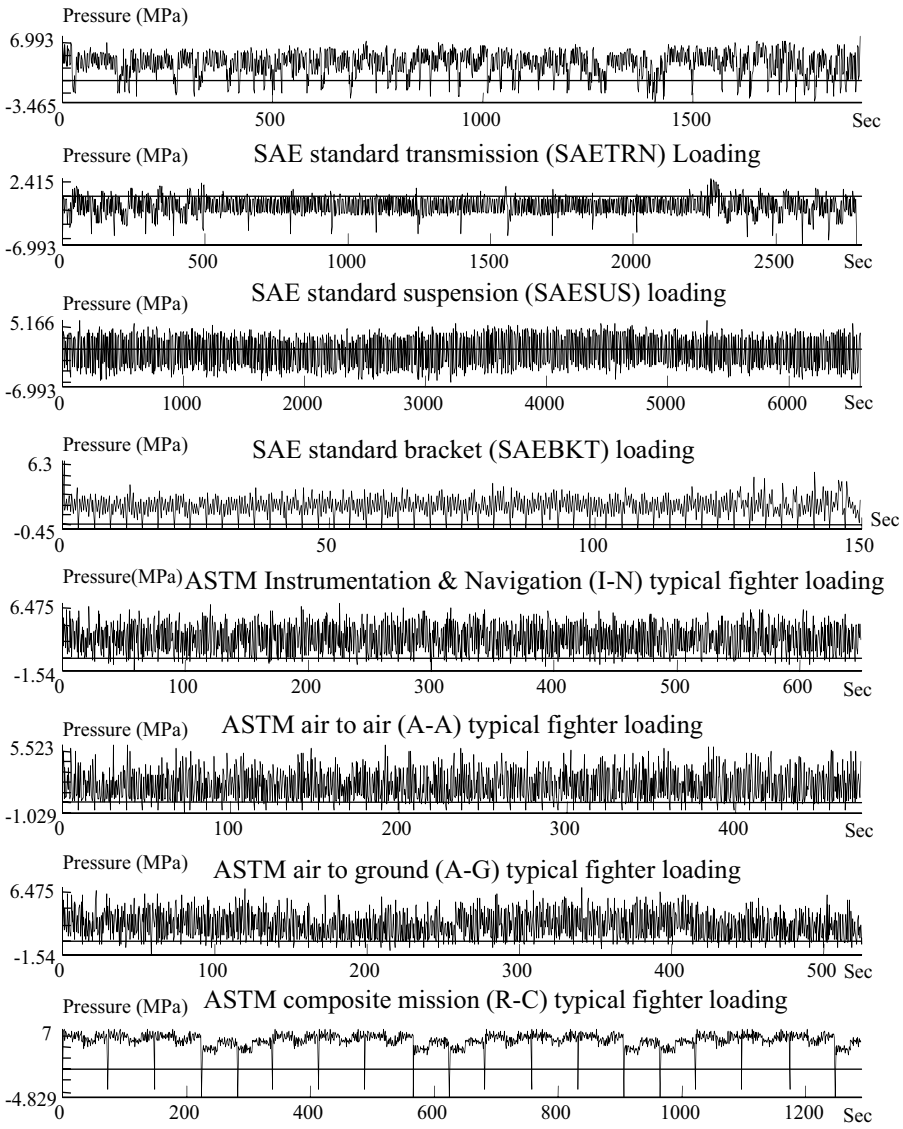

Figure 10 : Different time loading histories

produce residual compressive surface stresses. There are several available methods used to cold work the surface of a component to produce a residual compressive stress. The two most important are cold rolling and shot peening. These methods also known to produce the compressive residual stresses and harden the surface material. The significant improvement in fatigue life is due primarily to the generating residual compressive stresses. In shot peening process, the surface of the component undergoes plastic deformation due to the impact of many hard shots. The fatigue life of the component is improved due to the development of compressive residual stresses and the increase of hardness near the surface. The effect of surface treatment at different loading conditions for the polished vibrating cylinder block is summarized in Tab. 3. It is observed that the fatigue life for nitriding surface treatment is surprisingly higher than other surface treatment processes. Fig. 13 shows that the effect of different surface treatment processes for A-G loading conditions and polished specimen. It clearly shows that nitrided processes produce the highest fatigue life at critical location (node 49360, which produces the maximum stress and the minimum life) compare to other processes.

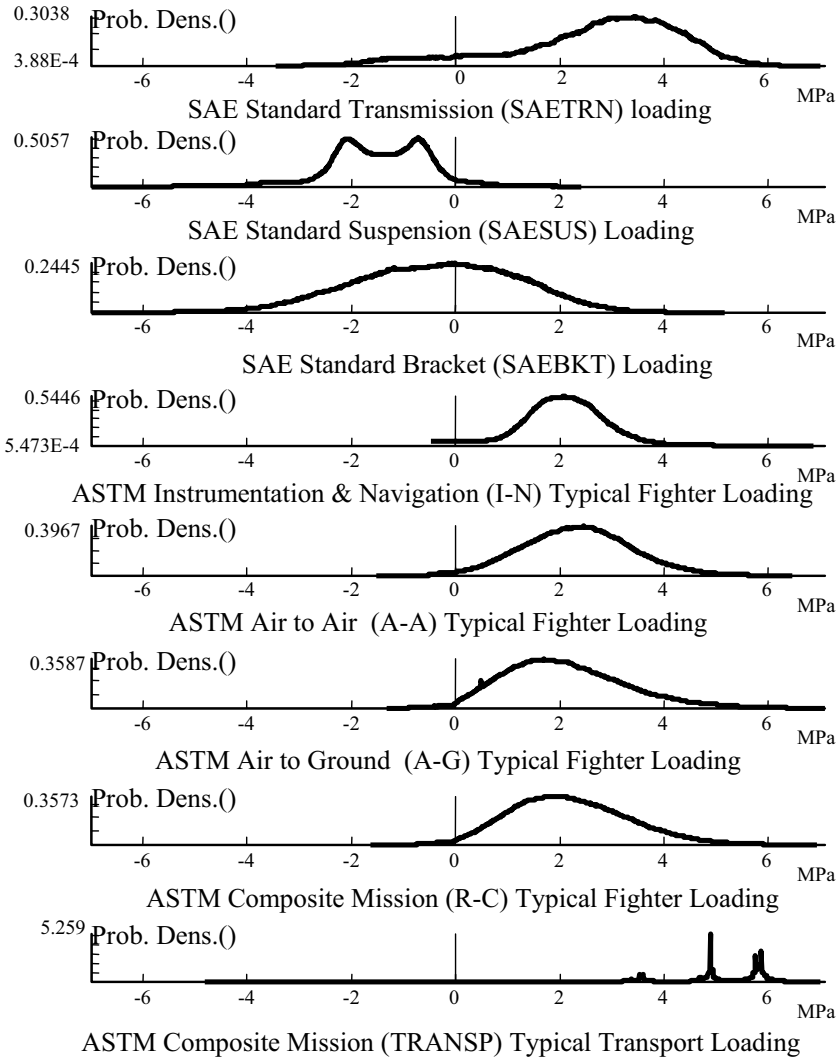

Figure 11 : Power spectral densities (PSD) responses

Table 3 : Effect of surface treatments at different loading conditions for polished components

Loading Conditions	Predicted life in seconds for different surface treatment processes			
	Nitriding	Cold rolling	Shot peening	Untreated
SAETRN	4.52×10^{10}	8.81×10^{8}	6.40×10^{7}	2.10×10^{7}
SAESUS	3.41×10^{6}	1.21×10^{14}	8.31×10^{11}	8.74×10^{10}
SAEBKT	8.08×10^{12}	5.31×10^{10}	1.68×10^{9}	4.06×10^{8}
I-N	6.35×10^{12}	3.68×10^{10}	1.01×10^{9}	2.30×10^{8}
A-A	2.77×10^{11}	2.92×10^{9}	1.40×10^{8}	3.93×10^{7}
A-G	1.84×10^{10}	3.51×10^{8}	2.52×10^{7}	8.23×10^{6}
R-C	7.21×10^{10}	1.02×10^{9}	6.01×10^{7}	1.83×10^{7}
TRANSP	2.40×10^{14}	9.55×10^{11}	1.33×10^{10}	2.27×10^{9}

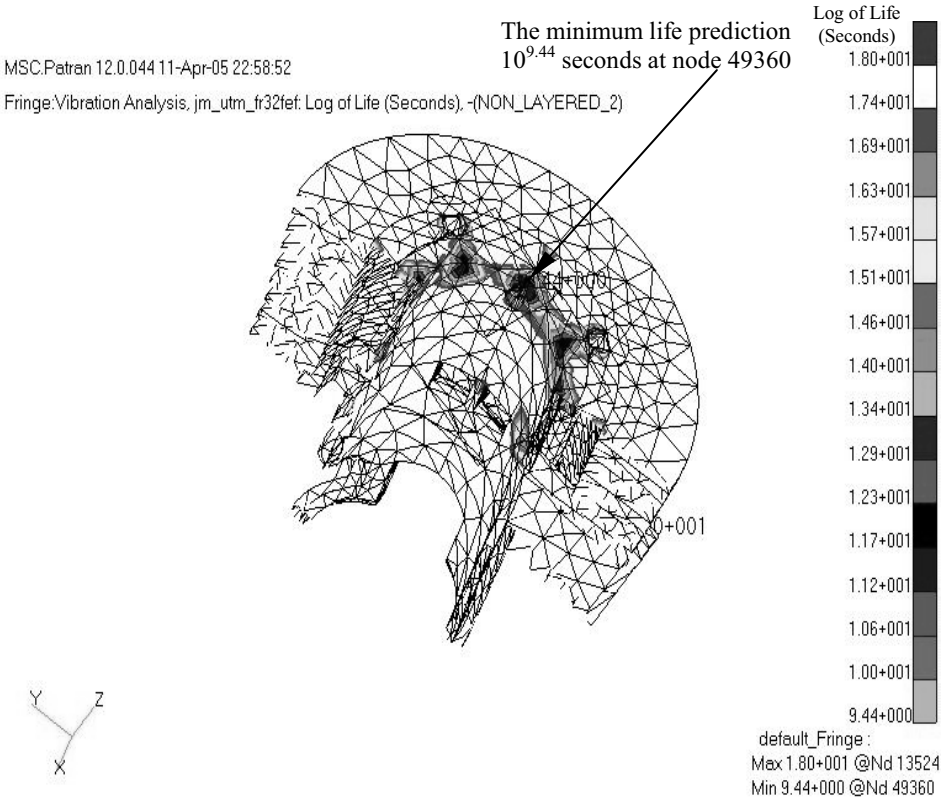

Figure 12 : Vibration fatigue life in log contour plotted for 32 Hz

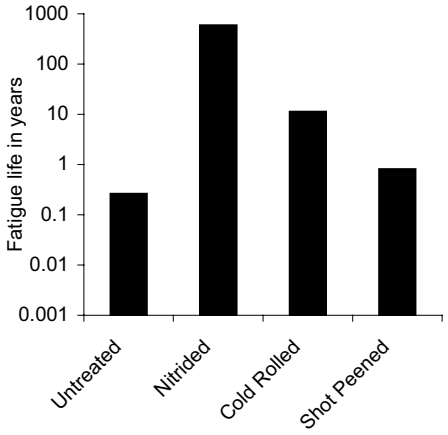

Figure 13 : Effect of different surface treatment processes for polished and A-G loading conditions.

7 Conclusions

The concept of spectral moments has been presented. A state of art of vibration fatigue techniques has been presented where the random loading and response are categorized using PSD functions. The Narrow band frequency domain fatigue analysis has been applied to a typical cylinder block of new two-stroke free piston engine. From the results, it can be concluded that compressive mean stress loading conditions gives the longest fatigue life for all materials. According to the results, all the surface treatment processes are capable of increasing the fatigue life of the aluminum alloys component. The surface residual compressive stress is found to have the greatest effect on the fatigue life. It can also be concluded that the combination of the polished and nitriding processes give the longest fatigue life of the cylinder block. Surface treatment to produce compressive forces in the outer layers of the component which will be cyclically loaded at stress raising locations. In addition, the vibration fatigue analysis can improve understanding of the system behaviors in terms of frequency characteristics of the structures, loads and their couplings.

Acknowledgement: The authors are grateful to Malaysia Government especially Ministry of Science, Technology and Environment under IRPA project (IRPA

project no: 03-02-02-0056 PR0025/04-03) for providing financial support.

References

Bannantine, S.A.; Comer, J.J.; Handrock, J.L. (1990): *Fundamentals of Metal Fatigue Analysis*. New Jersey, Prentice-Hall, USA.

Bendat, J. S. (1964): Probability Functions for Random Responses, *NASA report on Contract NASA-5-4590*.

Benedetti, M.; Fortanari, V.; Hohn, B. R.; Oster, P.; Tobie, T. (2002): Influence of shot peening on bending tooth fatigue limit of case hardened gears. *International Journal of Fatigue*, vol. 24**,** pp. 1127-1136.

Bishop, N. W. M.; Sherratt, F. (2000): *Finite element based fatigue calculations*, NAFEMS Ltd. UK.

Crandell, S.H.; Mark, W. D. (1973): *Random vibration in mechanical systems,* Academic Press, New York.

Formenti, D. (1999): The relationship between % of critical and actual damping in a structure. *Sound & Vibrations*, vol. 33, issue 4, pp. 14-18.

Gade, S.; Herlufsen, H.; Konstantin-Hansen H. (2002): How to determine the modal parameters of simple structures. *Sound & Vibrations*, vol. 36, issue 1, pp. 72-73.

Inoue, K.; Maehara, T.; Yamanaka, M. (1989): The effect of Shot peening on the bending strength of carburized gear teeth. *JSME Inter. Journal Series III*, vol. 32, issue 3, pp. 448-454.

Juvinall, R.C.; Marshek, K.M. (1991): *Fundamentals of Machine Component Design*. John Willey and Sons, New York, USA.

Kobayashi, M.; Matsui, T.; Murakami, Y. (1998): Mechanism of creation of compressive residual stress by shot peening. *International Journal of Fatigue,* vol. 20, issue 5, pp. 351-357.

Lipson, C.; Juvinall, R.C. (1963): *Handbook of Stress and Strength- Design and Material Applications*. Macmillan & Co., New York, USA.

Martin, U.; Altenberger, I.; Scholtes, B.; Kremmer, K.; Oettel, H. (1998): Cyclic deformation and near microstructures of normalized shot peened steel SAE 1045. *Materials Science and Engineering*, vol. A246, pp. 69-80.

MSC.Software. (2002): *User's Guide, Basic Dynamic Analysis*. MSC.Nastran version 68, MSC.Software Corporation, USA.

Newland, D.E. (1993): *An Introduction to random vibrations, spectral and wavelet analysis*. Longman Scientific and Technical, Essex, UK.

Novovic, D.; Dewes, R.C.; Aspinwall, D.K.; Voice, W.; Bowen, P. (2004): The effect of machined topology and integrity on fatigue life. *International Journal of machine Tools & Manufacture*, vol. 44, pp. 125-134.

Rahman, M.M.; Ariffin, A. K.; Jamaludin, N.; Haron, C.H.C. (2005): Analytical and finite element based fatigue life assessment of vibration induced fatigue damage. *The second International Conference on Research and Education in Mathematics (ICREM 2)*, Residence Hotel, Putrajaya, Malaysia, May 25-27, 2005, pp. 331-345.

Rahman, M.M.; Ariffin, A.K.; Jamaludin, N.; Haron C.H.C. (2005): Modeling and Analysis of Cylinder Block of Linear Generator Engine for Fatigue Durability. Proc. in the 4^{th} International Conference on Numerical Analysis of Engineering (NAE-2005), Hotel SANTIKA, Yogyakarta, Indonesia.

Reemsnyder, H.S. (1985): *Simplified Stress-life Model*. Bethleham steel Corporation report, Bethleham, PA.

Rice S.O. (1954): *Mathematical Analysis of Random Noise*, Selected papers on Noise and Stochastic processes, Dover, New York.

Rodopoulos, C.A.; Curtis, S.A.; Rios, E.R. de Los; SolisRomero, J. (2004): Optimisation of the fatigue resistance of 2024-T351 aluminum alloys by controlled shot peening – methodology, results and analysis. *International Journal of Fatigue*, vol. 26, pp. 849-856.

Schaeffer, H.G. (2001): *MSC.NASTRAN Primer for Linear Analysis*. MSC.Software Corporation, USA.

Stephens, R.I.; Fatemi, A.; Stephens, R.R.; Fuchs, H.O. (2001): *Metal Fatigue in Engineering*. John Wiley and Sons, Inc. , New York, USA.

Torres, M.A.S.; Voorwald, H.J.C. (2002): An evaluation of shot peening, residual stress and stress relaxation on the fatigue life of AISI 4340 steel. *International Journal of Fatigue*, vol. 24, pp. 877-886.

Tucker L.; Bussa S. (1977): *The SAE Cumulative Fatigue Damage Test Program: Fatigue under Complex Loading, Analysis and Experiments*. R.M. Wetzel, ed., SAE, Warrendale, PA, USA, **AE-6**: 1-54.

Wirsching, P.H.; Paez, T.L.; Oritz, K. (1995): *Random vibration, theory and practice.* John Wiley and Sons, Inc. USA.